Title

Dynamics of N_2O in vicinity of plant residues: a microsensor approach

By

Kyungmin Kim[1,2*], Turgut Kutlu[1], Alexandra Kravchenko[1,2], and Andrey Guber[1,2]

[1]Department of Plant Soil and Microbial Sciences, Michigan State University, East Lansing, MI 48823, U.S.A

[2]DOE Great Lakes Bioenergy Research Center, Michigan State University, East Lansing, MI 48823, U.S.A

Electronically submitted to:

Plant and Soil through Springer Editorial system

1/28/2021

[*]To whom correspondence should be addressed;

Email: kimkyu46@msu.edu

Phone: +1-626-679-8599

Fax: 517-355-0270

Keywords

Zymography, N_2O hotspot, Detritusphere, Plant decomposition, Switchgrass, β-glucosidase, Water absorption

Abstract

Aims Plant residues decomposing within the soil matrix are known to serve as hotspots of N_2O production. However, the lack of technical tools for microscale in-situ N_2O measurements limits understanding of hotspot functioning. Our aim was to assess performance of microsensor technology for evaluating the temporal patterns of N_2O production in immediate vicinity to decomposing plant residues.

Methods We incorporated intact switchgrass leaves and roots into soil matrix and monitored O_2 depletion and N_2O production using electrochemical microsensors along with N_2O emission from the soil. We also measured residue's water absorption and b-glucosidase activity on the surface of the residue - the characteristics related to microenvironmental conditions and biological activity near the residue.

Results N_2O production in the vicinity of switchgrass residues began within 0-12 hours after the wetting, reached peak at ~0.6 day and decreased by day 2. N_2O was higher near leaf than near root residues due to greater leaf N contents and water absorption by the leaves. However, N_2O production near the roots started sooner than near the leaves, in part due to high initial enzyme levels on root surfaces.

Conclusion Electrochemical microsensor is a useful tool for in-situ micro-scale N_2O monitoring in immediate vicinity of soil incorporated plant residues. Monitoring provided valuable information on N_2O production near leaves and roots, its temporal dynamic, and the factors affecting it. The N_2O production from residues measured by microsensors was consistent with the N_2O emission from the whole soil, demonstrating the validity of the microsensors for N_2O hotspot studies.

51

52 **Abbreviations**

53 MUF: 4-Methylumbelliferone

54 PAS: Photoacoustic Spectroscopy

55 Substrate: 4-Methylumbelliferyl-β-D-Glucoside

56 UV: Ultraviolet

57

58 ## Introduction

59 Nitrous oxide (N_2O) efflux from agricultural soils is highly spatially and temporally variable (Smith
60 and Tiedje, 1979; Goodroad et al., 1984; Parsons et al., 1991). Plant detritus, i.e., residues of plant roots
61 and aboveground biomass incorporated within the soil matrix, play an important role as originators of
62 'hotspots' of N_2O production and are in part responsible for high variability of N_2O fluxes (Parkin, 1987;
63 Garcia-Ruiz and Baggs, 2007). Such hotspots occur due to stimulation of microbial activity by the residues,
64 which are abundant sources of carbon (C) and nitrogen (N). The hotspots possess greater microbial biomass,
65 microbial diversity, and enzyme activity compared to the bulk soil, i.e., the soil not directly affected by
66 plant residues (Kuzyakov and Blagodatskaya, 2015).

67 In the bulk soil, oxygen (O_2) (Khalil et al., 2004), C (Myrold and Tiedje, 1985; Miller et al., 2008;
68 Senbayram et al., 2012), and N availability (Beauchamp, 1997; Blackmer and Bremner, 1978; Senbayram
69 et al., 2012; Wu et al., 2018) are known to be major factors regulating overall N_2O production. In soil
70 microenvironment adjacent to the residues, C, N and O_2 availability can be different from that in the bulk
71 soil. Contents of C and N are higher within 4-6 mm distance from the decomposing residues, due to
72 diffusion of decomposition products (Gaillard et al., 1999; Gaillard et al., 2003). Increased microbial
73 respiration stimulated by utilization of the nutrients reduces O_2 near the residues (McKenney et al., 2001;
74 Miller et al., 2008; Chen et al., 2013). Water absorption by the residues from the surrounding soil can
75 contribute to lower O_2 within the residue and in the surrounding detritusphere (Kravchenko et al., 2017;

Kim et al., 2020). The local anoxia stimulates denitrification, thus increases N_2O production (Miller et al., 2008; Li et al., 2016; Kravchenko et al., 2017). However, how fast the O_2 depletion occurs near the residue, and how it affects the magnitude of N_2O production within the residue are still unknown. Moreover, what are the main factors that determine the magnitude of N_2O production from these plant residue-induced hotspots is not fully understood.

One of the reasons for lingering poor understanding of N_2O production from residue-induced hotspots is a common reliance on the use of ground plant materials, which are typically well mixed with the soil, in experimental soil N_2O studies. In an intact soil, spatial distribution of residue fragments is highly heterogeneous and is known to be a crucial source of microscale resource heterogeneity (Loecke and Robertson, 2009). Mixing ground residues with the soil changes surface area of the residue, its contact with the soil, and the volume of the soil directly affected by the decomposing residues, leading to potentially significant discrepancies between the experimental results and what actually happens under field conditions (Kravchenko et al., 2018). Hence, work with intact residue fragments is essential for the studies of residue driven N_2O hotspots.

Another impediment to understanding the drivers of N_2O production in the residue-induced hotspots is a lack of tools for measuring O_2 depletion and N_2O production in close proximity to the residue. As a result, field as well as laboratory studies typically measure only the N_2O emitted into the atmosphere from the entire body of the sampled soil, not the N_2O produced within the individual hotspots. Electrochemical microsensors allow *in-situ* non-destructive measurements of gas concentrations with fast response time. They have been used to examine spatial and temporal dynamics of O_2 and N_2O in biofilms (Nielsen et al., 1990; Dalsgaard and Revsbech, 1992), rhizosphere (Revsbech et al., 1999), soil aggregates (Højberg et al., 1994), sediments (Meyer et al., 2008) and soil profiles (Hansen et al., 2014; Liengaard et al., 2014) in μm to mm scales. Due to high spatial resolution, microsensors can conduct measurements in specific microsites within soil matrix and, potentially, in vicinity to individual fragments of decomposing plant residues. However, they have never been used before for such purpose.

Moreover, with few exceptions (Højberg et al., 1994), experiments with N_2O and O_2 microsensors have been conducted primarily under fully saturated soil conditions (Jørgensen and Elberling, 2012; Hansen et al., 2014; Liengaard et al., 2014). The reason is that i) the anaerobic environment of fully saturated soils is favorable to denitrification and maximizes N_2O, and ii) the microsensor measurements are more stable and reliable in saturated conditions. However, N_2O emissions from the soil can be substantial even in aerobic conditions, partly due to denitrification within decomposing plant residues (Li et al., 2016; Kravchenko et al., 2017). Thus, the use of microsensors in unsaturated soil with incorporated intact residue fragments can generate new insights into this important component of soil N_2O emission. In contrast to initial N_2O microsensors that required completely anoxic conditions to measure N_2O precisely (Revsbech et al., 1988), recent electrochemical N_2O microsensors (Unisense A/S, Arhaus, Denmark) can measure both dissolved and gaseous N_2O with a detection limit of < 0.5 $\mu mol \cdot L^{-1}$ (μM). Yet, the question is how reliable and informative the data from these microsensors will be in vicinity to potential residue-induced N_2O hotspots in unsaturated soil.

The objective of this study was to evaluate the occurrence and temporal patterns of N_2O production in immediate vicinity to switchgrass (*Panicum Virgatum*) leaf and root residues incorporated into the soil. Within the homogenized soil of our experimental setup, the intact switchgrass residues were expected to serve as the primary nuclei for hotspots of N_2O production. We hypothesized that the patterns of N_2O production will depend on the residue characteristics. We emulated the situation when the activity of such hotspots is maximized, that is, when dry soil containing the residue is subjected to a wetting event. We also created soil moisture and pore-size distribution settings which were previously found to be optimal for promoting strong N_2O production from plant residue-induced hotspots (Kravchenko et al., 2017).

Our study aimed at addressing the following research questions: 1) How soon after the wetting the enhanced N_2O production at the surface of the residue begins? 2) How long the enhanced production lasts? 3) How well the N_2O levels in the vicinity of the plant residue-induced hotspots are related to the O_2 levels

and N_2O emissions from the soil into the atmosphere? 4) How water absorption and enzyme activity of the plant residues affect the N_2O production dynamics?

Methods

Soil and plant residues

Soil and plant materials were collected from a field where switchgrass was grown in monoculture since 2008 as part of the Great Lakes Bioenergy Research Center (https://lter.kbs.msu.edu/research/long-term-experiments/glbrc-intensive-experiment/) Biofuel Cropping System Experiment located at Kellogg Biological Station (Michigan, U.S.A). The soil of the experimental site is classified as Kalamazoo loam (mesic Typic Hapludalfs) developed on glacial outwash (Oates et al., 2016).

A composite soil sample was obtained from 5 randomly selected sites sampled at 5-10 cm depth. The collected soil was sieved through a 6 mm sieve to remove large stones and roots, and air-dried for a week. Air-dried soil was then sieved again to procure 1-2 aggregate fraction for the experiment. The decision to focus on the 1-2 mm aggregate fraction was driven by our previous findings that soil-incorporated plant residues made greater contribution to N_2O emissions when surrounded by the soil with prevalence of large pores, a setting that was the best achieved by using the large aggregate fraction (Kravchenko et al., 2017). The soil (1-2 mm fraction) was brought to 30% gravimetric water content level and pre-incubated for ~10 days at 20 °C. The purpose of pre-incubation was, first, to reduce the contribution of Birch effect of enhanced microbial activity in wetted soil, magnified in our experiment by previous soil disturbance and sieving (Negassa et al., 2015); and, second, to eliminate seedlings germinated from weeds present within the 1-2 mm soil fraction. The studied 1-2 mm fraction contained 0.97% total C, 0.095% total N, 0.17 mg N/kg of NO_3^-, and 2.05 mg N/kg of NH_4^+.

Switchgrass (var. Cave-in-rock) biomass was collected from 3 randomly selected sampling sites in October 2019. To minimize the disturbance, soil near switchgrass roots was removed by shovel and the entire plant body was plucked. In the laboratory, the plants were washed with distilled water and dried for

~3 weeks using a botanical press, leaves and roots separately. Dried and flattened leaves and roots were used for further analyses and experiments.

Microsensor experiment

Overview: The experimental setup consisted of two boxes (8.7x9.4x3.3 cm^3 each) filled with prepared 1-2 mm soil fraction with plant residues placed at a fixed position within each box (Fig. 1). To ensure the exact placement of the residues, a removable plastic frame was installed in the center of each box. The frame had a thin rectangular holder (area of 3.75 cm^2) in the center. Flattened plant residues were placed within the holder, the frame with the holder was installed in the box. Then two microsensors, one for N_2O and one for O_2 (N_2O-100 and OX-100 electrochemical microsensors with 100 μm tip, Unisense A/S, Aarhus, Denmark), were inserted through the openings on the side of the box. The microsensors were adjusted using the translation stage so as to ensure that the tips of both microsensors were in the immediate vicinity of each other and the surface of the residue (Fig. 1c). The openings through which the microsensors were inserted had a rubber cover that eliminated air flow into the box after the microsensors were in place. Lastly, the box was filled with 100 g of the prepared soil to reach ~1 $g \cdot cm^{-3}$ soil bulk density.

The top of the box was covered by an air-impermeable chamber with 30 ml headspace volume equipped with outlets for measurements of CO_2 and N_2O emissions from the surface of the soil. After assembling the chambers, the microsensor monitoring in the dry soil was conducted for approximately 3-4 hours. Then 30 mL of water was slowly added with a syringe from the top of the box to bring soil water content to 30% gravimetric content. Monitoring continued for subsequent ~5 days with every-minute microsensor readings and daily measurements of headspace N_2O and CO_2 using Photoacoustic Spectroscopy (PAS, INNOVA Air Tech Instruments, Denmark) using static chamber approach with a day interval for 5 days. We referred to the measurements next to the residue by the microsensors as N_2O production, and to the readings by PAS from the headspace above the soil samples as N_2O emission.

Experimental design: The experiment was a randomized complete block design with 8 replications, that is, 8 runs. Each run included two identically equipped and monitored boxes. One box contained leaf

175 residues and the other box contained root residues. In each run, the residues were assigned to the boxes at
176 random. Because of sensor malfunctioning, only the first 4 runs produced useable O_2 data.
177 *Residue preparation*: For leaf monitoring, multiple flattened switchgrass leaf fragments were
178 placed within the holder with minimal overlap. Each fragment was ~20 mm in length and 5-8 mm in width
179 (a typical width of the switchgrass leaves), with fragments for each experimental run cut from the same
180 plant (Fig. 1a). For root monitoring, multiple flattened plant roots with diameters ranging from 0.1 to 1 mm
181 and length of ~20 mm were placed within the holder.
182 *Sensor calibration*: The sensors were calibrated before and after every experimental run. A two-
183 point calibration was used for OX-100 sensors. The first calibration point (0 μM) was obtained in anoxic
184 solution of sodium ascorbate and NaOH, and the second point (283.03 μM) was obtained in the air-aerated
185 solution of DI water as described in the sensor manual (Oxygen Sensor User Manual,
186 https://www.unisense.com). A four-point calibration at N_2O concentrations of 0, 25, 50 and 100 μM was
187 used for the N_2O-100 sensors. The solutions were prepared by diluting N_2O - saturated water, which was
188 obtained by passing pure N_2O through DI water.
189
190 *Microsensor data processing*
191 After calibration, the data were filtered to remove the noise in the microsensor readings. The filtering
192 was conducted as following: 1) Medians and standard errors were calculated for every 100-minute interval
193 of the microsensor readings. 2) Only the readings within the range of median ± standard error were selected
194 for further analyses. All O_2 observations were adjusted to 320 μM of O_2 at the point of water addition,
195 which was the average value of O_2 in the dry soil. N_2O observations were adjusted so as to be set equal to
196 0 μM of N_2O at the time of water addition. Data processing was performed using pandas library (Available
197 at http://pandas.pydata.org/) in Python 3.6 (Python Software Foundation, available at
198 http://www.python.org/).

Three quantitative variables were derived from the adjusted N_2O microsensor measurements: peak N_2O production, time elapsed from the start of the soil wetting until the peak production, and cumulative N_2O productions. In most samples the concentration of N_2O increased after water addition and decreased after reaching the peak. In case of multiple peaks, the highest peak was used (e.g., Fig. 2 leaf rep4&5). The time between water application and the peak of N_2O production was referred to as a 'lag'. The values of peaks and lags for microsensor data records from all individual soil boxes are marked with black dotted lines in Fig. 2. Cumulative N_2O production was calculated as the area under the microsensor curves and above zero. For O_2, cumulative O_2 depletion was calculated as the area under the base O_2 concentration (320 μM). Cumulative N_2O production was calculated for 1 day, 2 day, and 3 day periods to enable comparisons with N_2O emission data, which were collected daily. The N_2O production and emission were the highest on day 1 and were substantially reduced in most samples by the end of day 2, thus no cumulative N_2O calculations after day 3 were performed for subsequent days.

Plant analysis

Switchgrass leaves and roots were subjected to water absorption measurements, zymography analysis, and total C and N measurements. Plant materials air-dried in the botanical press as described above were used for all the measurements.

Water absorption by residue: Water absorption by leaves and roots incorporated into the soil was measured by placing plant residues (n=3) of the known mass within the wet soil, allowing them to equilibrate, and then determining their weight gains. Specifically, 4 g of dry soil was packed in 5 cm Ø cylinder, and soil water content was adjusted to 30% gravimetric soil water content, the level consistent with that used in the microsensor experiment. Then, ~ 12.8 mg of dry switchgrass residue was placed in a single layer on the surface of the soil, covered by another 4 g of soil, and more water was added to bring the top soil to 30% gravimetric water content. The amount of residue added to soil was such as to ensure that the surface area of the incorporated material was equal to ~3 cm^2. After 4 hours of equilibration, the

soil cylinders were disassembled; the residues were retrieved, cleaned from small soil particles attached to the surface with a brush, and weighed. The increase in the residue weight reflected the amount of water absorbed by the residue from the surrounding soil.

β-glucosidase activity on residue surfaces: Spatial distribution of the β-glucosidase on the surface of the soil-incorporated leaves and roots was measured using zymography (Spohn et al., 2013; Guber et al., 2019). In a course of zymography, a membrane saturated with an enzyme-specific substrate is placed on the surface of the studied material (e.g., soil). The substrate diffuses from the membrane into the soil where a contact with the enzyme results in the substrate decomposition and a release of the fluorescent product. The map of the products distribution on the membrane is visible in ultraviolet (UV) light and is representative of the enzyme activities on the studied surface.

Soil and residue packing procedure for zymography was similar to that of the water absorption experiment. Specifically, a 15 g of 1-2 mm soil fraction was packed in a 4.7*2* 3.3 cm^3 soil box, and soil water content was adjusted to 30% (gravimetric). Then, ~ 30 mg of dry switchgrass residue was placed on top, covered by another 15 g of soil, and more water was added to bring the top layer of soil to 30%. Soil boxes were placed into 500 mL Mason jars, with 8 mL of distilled water added on the bottom to prevent soil drying; and incubated for 3 days at 20 ° C in the dark (n=2). Each soil box was taken out of the Mason jar twice during the incubation, on day 1 and day 3, to take zymography images. For that, one side of the box (4.7 * 3.3 cm^2) was opened, and a 4*3 cm^2 polyamide membrane filter (0.45 μm; Tao Yuan, China) soaked in 6 mM solution of 4-Methylumbelliferyl-β-D-Glucoside (Substrate) was placed on top of the soil surface. Substrate is the fluorogenic solution specific to β-glucosidase, which contains florescent product (4-Methylumbelliferone, MUF) which can be cleaved by enzymes, and fluorescence intensity is then used to calculate β-glucosidase activity. Soil surface with the membrane filter was photographed every 5 minutes for 40 minutes in total under the UV light, using Canon EF 75-300 mm f/4-5.6 III Telephoto Zoom Lens (Canon U.S.A. Inc., U.S.A).

For calibration of florescence intensity, 5 μL of MUF standard solutions with concentrations of 1, 2, 5, 10, 50, 100 μM were added to 1 cm^2 membranes and photographed in the UV light with camera setting described above. The parameters of nonuniform calibration were calculated as described in Guber et al. (2019). All zymography images were corrected for the background intensity by subtracting the first image. Then corrected zymography images were converted to MUF contents using the calibration parameters. Time series of MUF contents on the images were used to calculate the enzymatic activities in the membrane pixels. The activity was calculated as a maximum slope of linear parts of MUF time series (9 points for 40 mins). The 0.27 cm^2 wide area encompassing the residue was used to quantify the enzyme activity on the residues (Fig. 3).

Total C and N values of the residues: Total C and N of switchgrass leaves and roots were measured using an Elemental Analyzer (ECS 4010 CHNSO Analyzer, Costech Analytical Technologies Inc., U.S.A) (3 replicates). Approximately 15-20 mg of the residue was used for each replicate sample. The residues were cut into small pieces (< 1 mm) using surgical scissors before being packed in the tin caps for the C and N measurements.

Statistical analysis

Data analyses for comparisons between the residue types were conducted using PROC MIXED procedure (SAS 9.4, SAS Institute Inc., U.S.A) following recommendations by Milliken and Johnson (2009). For all quantitative variables derived from the microsensor N_2O observations, e.g., peak N_2O production, lag, and cumulative N_2O production, the statistical models consisted of the fixed effect of the residue type (leaves and roots) and random effects of the experimental run and the sensor ID.

The statistical model for the analysis of N_2O and CO_2 emissions in the headspace air above the soil boxes from PAS consisted of residue type, day since water addition, and their interaction as fixed effects; and the experimental run and run by the residue type interaction as random effects. The latter was used as an error term for testing the main effect of the residue type. Repeated measures approach was used to

account for repeated measurements of N_2O and CO_2 from the same soil box during the experiment. The optimal variance-covariance structure was determined as such that produced the lowest AIC and BIC values (Milliken and Johnson, 2009). For both N_2O and CO_2, first-order autoregressive covariance structure was used in the final model.

The statistical model for the analysis of the enzyme activity data consisted of residue type, day, and their interaction. Repeated measures approach was used here as well, using the same model selection approach as described above for $N_2O \cdot CO_2$ data analysis. The model with unequal variances per day was used as the final model. Since the interaction between the residue type and day was significant, we conducted "slicing", a.k.a simple effect testing, of the interaction by day and by residue type. When the simple effect F-test was found to be statistically significant, comparisons among the days within each residue type were performed using t-test.

Relationships among the studied continuous variables, e.g., residue mass and N_2O production, N_2O production and N_2O emission, were studied using regression analysis with PROC REG in SAS. To examine the difference in regression slopes between the two residue types, we used PROC MIXED with model consisting of the residue type effect and the interaction between the residue type and the residue mass, the latter as a continuous variable. Replication and sensor ID were considered as random factors.

For all statistical models, the assumption of normality was checked by examining normal probability plots. When the normality assumption was violated, the original data was log-transformed. Equal variance assumption was checked using Levene's test based on absolute residuals. When violated, we examined potential unequal variance models, and the models with the lowest AIC and BIC values were selected for further analyses. The results were reported as statistically significant when p-value was < 0.05 and as trends when p-value was < 0.10; and marked with * ($p < 0.10$), ** ($p < 0.05$), and *** ($p < 0.01$).

Results

Microsensor experiments

298 After adding water, O_2 concentration near both leaf and root residues decreased immediately or
299 within 12 hours (Fig. 4a). In all 4 replications of root residues, O_2 levels became stable soon after the initial
300 drop, reaching to ~280 μM. This L-shape trend of O_2 dynamics in the samples with root residues was not
301 different from that of the control soil (with no residue added, data from preliminary experiment) (Fig. 4a).
302 However, it was not always the case in the samples with leaf residues. In two of the four replications of leaf
303 residue, O_2 levels further decreased after the initial immediate decrease and reached minimums of 50-150
304 μM at ~ 1.5 day after water addition. In the other two samples, O_2 remained stable after the initial decrease,
305 similar to the root samples.
306 In 10 out of total 16 replicated samples, N_2O concentration near the residues increased immediately
307 after the water addition (Fig. 2; Leaf rep 1, 3, 4, 5, 6, and Root rep 1, 3, 5, 6, 8). In the remaining 6 samples
308 (Leaf rep 2, 7, 8, and Root rep 2, 4, 7), N_2O concentration started to increase within 12 hours. Typically,
309 the N_2O increases occurred almost simultaneously with the drastic drops in O_2 concentrations. The time
310 elapsed until reaching the maximum N_2O production (i.e., lag) was twice longer for leaf as compared to
311 root residues (0.92 vs. 0.41, $p < 0.05$, Fig. 5d). Both the peak and the cumulative N_2O productions were
312 significantly higher in leaf residues compared to root residues ($p < 0.05$, Fig. 5a, b). Peak and cumulative
313 N_2O productions were strongly positively correlated ($p < 0.01$, Fig. S1a).
314 Across both residue types, greater mass of the residue resulted in higher peaks of N_2O production
315 (Fig. S1b). The positive trend was present in the leaf residue, where a 1 g of increase in leaf mass resulted
316 in a 12.3 μM increase in N_2O peak production ($p < 0.10$), however one observation point with an
317 exceptionally high peak N_2O production was excluded from this analysis. The residue mass did not affect
318 peak N_2O production in the root residues. The residue mass and cumulative N_2O production were not
319 significantly correlated, likely due to high variability of the latter (results not shown). N_2O production was
320 significantly and positively correlated with cumulative O_2 depletion ($p < 0.10$, Fig. 4b).
321 N_2O emissions from the soil displayed similar patterns to N_2O microsensor observations. The
322 emissions were the highest on day 1 (Fig. 6). N_2O emissions from the samples with leaves were numerically

323 higher than those from the samples with roots through the first 5 days of incubation, but the difference
324 tended to be statistically significant only on day 1 ($p < 0.10$). The differences between leaves and roots in
325 terms of CO_2 emission rates were not statistically significant. The CO_2 and N_2O emissions were positively
326 related ($p < 0.01$, Fig. S2), and the relationship between them was stronger in root ($R^2=0.57$) than in leaf
327 ($R^2=0.41$) residue samples. Cumulative N_2O production and cumulative N_2O emission also were positively
328 correlated to each other for day 1, day 2, and day 3 of the experiment (Fig. 7).
329
330 *Plant analysis*
331 Both leaf and root residues absorbed significant amount of water from the surrounding soil (Fig.
332 8a). Leaves absorbed ~1.4 g of water per each g of air-dry biomass, while roots only absorbed 1 g of water
333 per g of biomass ($p < 0.10$, Fig. 8a). Root residues had more C but less N than leaves, resulting in contrasting
334 C:N ratios between the two (24.0 vs. 82.7, Table 1).
335 Average β-glucosidase activities from the surface of the residues are presented in Fig. 8b. At the
336 first day of the experiment, the enzyme activity was more than 40 times higher on root as compared to leaf
337 surfaces. However, by day 3 the β-glucosidase activity on roots substantially decreased while on leaves it
338 increased, resulting in no statistical differences between the residue types.
339
340 **Discussion**
341 Our study demonstrated the utility of the microsensors in monitoring the O_2 and N_2O levels in
342 immediate vicinity to the soil incorporated plant-residues, which are known originators of N_2O hotspots
343 (Parkin, 1987). The study provided the answers to the research questions we posed. In the conditions
344 optimal for both microbial activity and gas diffusion, that is, at 48% water-filled pore space (WFPS) and in
345 abundant presence of large air-filled soil pores of this study, the N_2O is quickly emitted out of the soil in
346 the amounts positively associated with its production (Fig. 7). Yet, the strength of the association between
347 the N_2O near the residues and that emitted into the atmosphere deteriorates over time, reflecting the short-

348 lived nature of the residue hotspots' contribution to the emissions. The origin of the hotspot, i.e., leaves vs.
349 roots, affects the magnitude of the production and emission as well as their temporal dynamic (Figs. 2 and
350 6).
351
352 *Effect of incorporated switchgrass leaves and roots on N_2O production and emission*
353 Greater amounts of N_2O produced (for 2 days) from incorporated leaves than roots (Fig. 5b) result
354 from lower C:N ratio and higher N contents of the portions of leaf residues readily available to microbial
355 decomposers. While here we only measured total C and N plant contents (Table 1), marked differences
356 between leaves and roots, especially, in terms of total C:N ratio, suggest that similarly contrasting
357 differences likely occurred in labile portions of the plant tissues. While low C:N ratio in residues can
358 promote mineralization, high C:N ratio can lead to N immobilization, reducing N_2O emissions (Miller et
359 al., 2008). Also, microorganisms can utilize C and N from leaves more efficiently than those from the roots
360 (Garcia-Ruiz and Baggs, 2007; Partey et al., 2014). Though not measured in this study, contrasting organic
361 chemistry of leaves and roots likely played a role as well. Higher soluble organic C and N in the leaves are
362 known to result in rapid decomposition, while higher concentration of cellulose, bound phenols and lignin
363 phenols in roots can retard decomposition (Birouste et al., 2012; Uselman et al., 2012; Wang et al., 2015).
364 The soil used in this study had low total C, total N, and inorganic N levels compared to the residue,
365 indicating that the N_2O production in our soil samples was primarily driven by the microbes that relied on
366 the readily available substrates from the residues, not soil, as their main energy source. Thus, leaves, which
367 provided more available nutrients resulted in greater N_2O production. These results are in line with previous
368 studies reporting positive correlations between available C and denitrification (Myrold and Tiedje, 1985;
369 Miller et al., 2008).
370 While it was expected that greater size of the incorporated residue would be associated with greater
371 N_2O production (Garcia-Ruiz and Baggs, 2007), that trend was significant only in leaf residue samples (Fig.
372 S1b). We attribute this result in part to a narrower range of root mass compared to leaf mass - as the roots

373 used in the study tended to weigh somewhat less than the leaves. Differences in residue chemistry between
374 leaves and roots also likely contributed to the observed differences in correlation strengths. Larger water
375 absorption was another factor that contributed to higher N_2O production in the leaves (Fig. 8a), as it
376 stimulated development of anoxic conditions and denitrification (Kravchenko et al., 2017).

377 Greater N_2O production near the leaves translated into higher N_2O emissions during the first day
378 of incubation (Fig. 6a). However, afterwards the difference between the leaves and roots disappeared,
379 consistent with an overall decrease in the strength of the association between N_2O near the residues and the
380 emitted N_2O (Fig. 7) and pointing to the reduced importance of the residue's contribution to N_2O emissions.
381 It is also possible that the reduction of N_2O to N_2 contributed to the decreased association between produced
382 and emitted N_2O. However, the relatively large (> 30 μm) air-filled pores dominating soil pore-size
383 distribution of the studied soil (Toosi et al., 2017) are unlikely to cause complete anoxic conditions within
384 the soil. The final denitrification product is expected to be N_2O rather than N_2 when the oxygen in the pore
385 is sufficient (Hwang and Hanaki, 2000). Most of produced N_2O likely quickly escaped through the air-filled
386 pores, contributing to the positive relationship between N_2O production and emission. It contrasts other
387 works which used fully saturated soils and reported delays in N_2O emission (Markfoged et al., 2011).

388 While the CO_2 and N_2O emissions were positively correlated in both leaves and roots (Fig. S2),
389 variations in CO_2 emissions explained 57% of variations in N_2O emissions in the root residues, while only
390 41% in the leaf residue samples (Fig. S2). Positive correlations between CO_2 and N_2O emissions reflect
391 stimulated microbial activity in both CO_2 and N_2O production (Azam et al., 2002; Millar and Baggs, 2004),
392 and the role of C utilization due to increased microbial activity in N_2O production (De Catanzaro and
393 Beauchamp, 1985; Millar and Baggs, 2004; Hayashi et al., 2015). Weaker association between CO_2 and
394 N_2O in the leaf residue samples further highlights the hotspot nature of the N_2O production within the soil
395 with incorporated decomposing leaves. Indeed, the anoxic conditions developed in response to greater water
396 absorption by the leaves (Fig. 8a) were conducive to denitrification and to resultant N_2O production and
397 emission, while unfavorable to CO_2 production.

398

399 *Effect of incorporated switchgrass leaves and roots on N_2O temporal dynamic*

400 On average, the N_2O levels near the root residues reached the peak level faster than near the leaves,
401 i.e., within 0.4 day and 0.8 day, respectively (Fig. 5d). A more rapid start of N_2O production in vicinity of
402 the roots probably resulted from a greater presence of inherent extracellular enzymes on the root surfaces
403 (Fig. 8b). The enzymes were produced by both the roots and soil microorganisms when the roots were alive
404 and remained since on the root surfaces (Razavi et al., 2016). Nagahashi and Baker (1984) showed that
405 even after the roots were dead, washed, and dried prior to incubation, β-glucosidase still remained on their
406 surfaces and was not readily removed by washing. Even in fumigated soil the extracellular enzymes retained
407 their activity for ~12 weeks (Schimel et al., 2017). Since β-glucosidase measured in this study is one of the
408 common enzymes produced by both roots and microorganisms, it can be regarded as an indicator of such
409 overall extracellular enzyme presence (Kang et al., 1998; Sinsabaugh et al., 2008; Cayuela et al., 2009).
410 When the roots were rewetted, the inherent enzymes were activated, and immediately started hydrolyzing
411 the residue. The enzymes remaining on the roots likely accelerated root decomposition, and led to
412 subsequently faster initiation of N_2O production, as compared to the leaves. This observation is consistent
413 with the earlier findings that preexisting denitrifying enzymes in the soil govern the initiation of
414 denitrification, while it takes ~6 hours until the enzymes are newly synthesized by microbes using energy
415 supplied from surroundings (Smith and Tiedje, 1979). Our study supports the importance of inherent
416 enzymes not only in the soil but also on the surfaces of decomposing roots.

417 The activity of inherent enzymes on the roots decreased by day 3, possibly because their
418 consumption rate was greater than the rate of new synthesis (Smith and Tiedje, 1979). Synthesis of new
419 enzymes by microorganisms is possible only when there are sufficient available nutrients (Allison and
420 Vitousek, 2005; Wallenstein and Weintraub, 2008). As indicated from total plant N content (Table 1), N
421 was not as readily available in the roots as in the leaves in our study, leading to low enzyme activity after
422 the inherent enzymes were consumed. Enzyme activity in the leaves, on the contrary, was low at the

beginning and significantly increased by day 3 (Fig. 8b), indicating new enzyme production, likely stimulated by higher levels of available N. Longer lag and greater peak of N_2O production in leaves seemed to be related to newly synthesized enzyme activity at the surface of the residues. Longer lag in the leaves as compared to roots is also attributable to the presence of epicuticular layer on the leaf surfaces that prevents the water loss (Bragg et al., 2020; Riederer and Schreiber, 2001; Yeats and Rose, 2013). The release of labile substrates might have been delayed by this hydrophobic layer, leading to the delay of the peak in leaf residues. While the peak N_2O production is a function of the amount of dissolved organic C and N, lag is likely more a function of the release rate of the dissolved organic matter from the residues.

O_2 at plant residue surfaces and its relationship with N_2O

We observed a weak tendency for O_2 near the residues to be more depleted in the leaf than in the root samples (Fig. 4a). In all root samples and 2 of the 4 leaf samples, the dynamics of O_2 concentrations near the residues was not substantially different from that of the control soil, suggesting that the changes in O_2 were caused by an inflow of water into the air-filled pore space of the initially dry soil samples, and not by the plant residue decomposition. It is also possible that O_2 sensor tips of these samples was placed in the air-filled large pores, thus could not reflect the overall O_2 changes near the residues. Yet, a marked decrease in O_2 that took place in 2 of the leaf residue samples following the initial drop suggested that enhanced leaf decomposition did lead to greater O_2 depletion near the leaves. Overall, leaves are known to decompose faster than roots due, in part, to their lower lignin:N ratios (Steffens et al., 2015) and lower C:N ratio (Edmonds, 1980; Baggs et al., 2000; Zhang et al., 2008) (Table 1). Faster decomposition is associated with greater microbial respiration and growth, thus greater O_2 consumption (Chen et al., 2013). Hence, these large decreases after O_2 reached the initial short plateau can be due to enhanced O_2 consumption occurred during leaf residue decomposition. Greater water absorption is possibly another potential contributor to greater O_2 depletion near leaf residues (Fig. 8a), since water absorption by the residue fragments can induce

higher water contents in their vicinity (~150 μm) (Kim et al., 2020), consequently, reducing O_2 concentrations (Kravchenko et al., 2017).

The lack of O_2 stimulates denitrification and promotes N_2O production (Castaldi, 2000; McKenney et al., 2001). We observed a simultaneous occurrence of O_2 depletion and N_2O production, and a positive correlation between the cumulative O_2 depletion and N_2O production ($p < 0.10$, Fig. 4b). It contrasts with Rohe et al. (2020) who did not find significant relationship between microsensor O_2 observations and denitrification (N_2O and N_2O+N_2). However, Rohe et al. (2020) conducted O_2 measurements at local microsites representing only 0.2% of the total soil volume, while they assessed denitrification from the entire soil samples. In our study N_2O and O_2 were measured in close spatial proximity to each other (<1 mm distance). The discrepancy between these two studies reflects high spatial variability of N_2O production and emphasizes the necessity of smaller-scale approach to understand N_2O hotspots.

Still, O_2 depletion explained only 25% of variation in N_2O production near the residues (Fig. 4b). One possible reason for the relatively weak association between O_2 and N_2O is that some of N_2O was produced via nitrification, which likely occurred in O_2 rich 48% WFPS experimental settings of our study. Although denitrification is responsible for production of more than 50% of N_2O in residue-incorporated soils, nitrification is another substantial source of N_2O (Li et al., 2016). Another possible reason is the complete denitrification of N_2O to N_2. Even though our experimental setup was designed to maximize the N_2O production and minimize its conversion to N_2, complete denitrification always occurs, and it is especially prominent when O_2 is depleted to less than 25% of the atmospheric level (Morley and Baggs, 2010). It corresponds to 75 μM O_2 concentration in our study, thus in the samples with leaves which had the greatest cumulative O_2 depletion (Fig. 4b), the relationship between O_2 and N_2O might have been weakened due to further denitrification.

Evaluation of microsensors as a tool for hotspot detection

Even under well-controlled experimental settings with precisely placed residues, sieved/preincubated soil, and stable temperature and humidity in the laboratory, there was still a substantial variability in microsensor measurements of O_2 depletion and N_2O production in vicinity of the residues (Fig. 5). The main cause of such variability are natural variations in characteristics of the hotspots themselves. Our experimental set up was designed so as to minimize the variations, i.e., we used sieved 1-2 mm soil fraction, which was cleaned of particulate organic fragments and stones and pre-incubated. Yet, the sizes, locations, water or air-filled status, and connectivity of pores in vicinity of each plant residue were not controllable. The development and activity of microbial hotspots can be significantly affected by these micro-scale conditions, leading to variations of O_2 depletion, N_2O production and emission.

Another possible cause is variability in microenvironmental conditions surrounding the microsensor tips. For example, after the microsensor was inserted and soil and water were added to the experimental box, it was not possible to confirm whether the sensor's tip ended up being within the water or in the air. The sensor's tip could have been covered by menisci of incoming water or it could have been located within a trapped air between soil aggregates. Depending on the location and the distance to air-filled atmosphere-connected pores, O_2 concentration measured by microsensors can be substantially different even within the same soil (Rohe et al., 2020). Placing sensor tips in certain positions within pores to observe the gas changes at the surface of residues is even more challenging, as implied by our highly variable O_2 depletion pattern in leaves. The microsensor's 100 μm-scale resolution measures the gas dynamics in a certain pore near the residue, and might not fully represent the dynamics occurring on the entire residue surface. Moreover, concentrations and fluxes in water and air are drastically different and not reflected by the gas partial pressure values – the actual data recorded by the microsensors. Our experiment stresses the difficulties in measurements of N_2O production, especially in unsaturated conditions of soil at a microscale.

Another peculiarity observed in microsensor performances in our study were occasional simultaneous fluctuations in the records from all operating microsensors (Fig. 2). The artificial nature of such fluctuations

was evident from identical patterns present simultaneously in N_2O and O_2 microsensors of both boxes. The artificial patterns were small compared to the peak measurements, thus non-detectable during the first 2 days of each experimental run, but they became visible when the microsensor readings decreased approaching atmospheric levels (Fig. 2). What induces such fluctuations and how to minimize them requires further investigation.

Despite discussed above limitations and difficulties, it should be emphasized that the use of microsensors enabled generating valuable information on N_2O production near the residue hotspots and on its temporal dynamic. The obtained information was consistent with the N_2O emissions measured using the traditional approach and agreed well with the effects of plant residue characteristics on N_2O production expected based on theoretical considerations and published literature. Our results emphasize the validity and usefulness of the microsensors for studies of soil N_2O production hotspots aimed at understanding mechanisms of micro-scale N_2O hotspot production.

Acknowledgements

We would like to thank Chelsea Mamott and GLBRC communication team for help with figure preparations. We also thank Dr. Dirk Colbry for help with data processing and Maxwell Oerther for assisting in laboratory work.

Funding

This work was funded in part by the National Science Foundation's Geobiology and Low Temperature Geochemistry Program (Award 1630399). Support for this research was provided by the Great Lakes Bioenergy Research Center, U.S. Department of Energy, Office of Science, Office of Biological and Environmental Research (Award DE-SC0018409), by the National Science Foundation Long-term Ecological Research Program (DEB 1832042) at the Kellogg Biological Station, and by Michigan State University AgBioResearch.

Conflicts of interest

Not applicable

Availability of data and material

Not applicable

Code availability

Not applicable

Author's contributions

A.K and A.G. designed and directed the project. T.K. and A.G. worked out technical details and performed calibrations for the microsensor experiment. All the authors performed the experiments. K.K., A.K., and A.G processed analyzed the data. All authors discussed the results and K.K. and A.K. wrote the manuscript.

Reference

Allison, S.D. and Vitousek, P.M., 2005. Responses of extracellular enzymes to simple and complex nutrient inputs. Soil Biology and Biochemistry. 37, 937-944.

Azam, F., Müller, C., Weiske, A., Benckiser, G., Ottow, J., 2002. Nitrification and denitrification as sources of atmospheric nitrous oxide–role of oxidizable carbon and applied nitrogen. Biology and fertility of soils 35, 54-61.

Baggs, E., Rees, R., Smith, K., Vinten, A., 2000. Nitrous oxide emission from soils after incorporating crop residues. Soil use and management 16, 82-87.

Beauchamp, E., 1997. Nitrous oxide emission from agricultural soils. Canadian Journal of Soil Science 77, 113-123.

Birouste, M., Kazakou, E., Blanchard, A. and Roumet, C., 2012. Plant traits and decomposition: are the relationships for roots comparable to those for leaves? Annals of Botany. 109, 463-472.

Blackmer, A., Bremner, J., 1978. Inhibitory effect of nitrate on reduction of N2O to N2 by soil microorganisms. Soil Biology and Biochemistry 10, 187-191.

Bragg, J., Tomasi, P., Zhang, L., Williams, T., Wood, D., Lovell, J.T., Healey, A., Schmutz, J., Bonnette, J.E. and Cheng, P., 2020. Environmentally responsive QTL controlling surface wax load in switchgrass. Theoretical and Applied Genetics. 133, 3119-3137.

Castaldi, S., 2000. Responses of nitrous oxide, dinitrogen and carbon dioxide production and oxygen consumption to temperature in forest and agricultural light-textured soils determined by model experiment. Biology and fertility of soils 32, 67-72.

555 Cayuela, M., Sinicco, T., Mondini, C., 2009. Mineralization dynamics and biochemical properties
556 during initial decomposition of plant and animal residues in soil. Applied Soil Ecology 41, 118-127.
557 Chen, H., Li, X., Hu, F., Shi, W., 2013. Soil nitrous oxide emissions following crop residue
558 addition: a meta- analysis. Global change biology 19, 2956-2964.
559 Dalsgaard, T., Revsbech, N.P., 1992. Regulating factors of denitrification in trickling filter
560 biofilms as measured with the oxygen/nitrous oxide microsensor. FEMS Microbiology Letters 101, 151-
561 164.
562 De Catanzaro, J., Beauchamp, E., 1985. The effect of some carbon substrates on denitrification
563 rates and carbon utilization in soil. Biology and fertility of soils 1, 183-187.
564 Edmonds, R.L., 1980. Litter decomposition and nutrient release in Douglas-fir, red alder, western
565 hemlock, and Pacific silver fir ecosystems in western Washington. Canadian Journal of Forest Research
566 10, 327-337.
567 Gaillard, V., Chenu, C., Recous, S., 2003. Carbon mineralisation in soil adjacent to plant residues
568 of contrasting biochemical quality. Soil Biology and Biochemistry 35, 93-99.
569 Gaillard, V., Chenu, C., Recous, S., Richard, G., 1999. Carbon, nitrogen and microbial gradients
570 induced by plant residues decomposing in soil. European Journal of Soil Science 50, 567-578.
571 Garcia-Ruiz, R., Baggs, E., 2007. N 2 O emission from soil following combined application of
572 fertiliser-N and ground weed residues. Plant and Soil 299, 263-274.
573 Goodroad, L., Keeney, D., Peterson, L., 1984. Nitrous oxide emissions from agricultural soils in
574 Wisconsin. Journal of Environmental Quality 13, 557-561.
575 Guber, A.K., Kravchenko, A.N., Razavi, B.S., Blagodatskaya, E., Kuzyakov, Y., 2019.
576 Calibration of 2- D soil zymography for correct analysis of enzyme distribution. European Journal of Soil
577 Science 70, 715-726.
578 Hansen, M., Clough, T.J., Elberling, B., 2014. Flooding-induced N2O emission bursts controlled
579 by pH and nitrate in agricultural soils. Soil Biology and Biochemistry 69, 17-24.
580 Hayashi, K., Tokida, T., Kajiura, M., Yanai, Y., Yano, M., 2015. Cropland soil–plant systems
581 control production and consumption of methane and nitrous oxide and their emissions to the atmosphere.
582 Soil science and plant nutrition 61, 2-33.
583 Højberg, O., Revsbech, N.P., Tiedje, J.M., 1994. Denitrification in soil aggregates analyzed with
584 microsensors for nitrous oxide and oxygen. Soil Science Society of America Journal 58, 1691-1698.
585 Hwang, S. and Hanaki, K., 2000. Effects of oxygen concentration and moisture content of refuse
586 on nitrification, denitrification and nitrous oxide production. Bioresource Technology. 71, 159-165.
587 Jørgensen, C.J., Elberling, B., 2012. Effects of flooding-induced N2O production, consumption
588 and emission dynamics on the annual N2O emission budget in wetland soil. Soil Biology and
589 Biochemistry 53, 9-17.
590 Kang, H., Freeman, C., Lock, M., 1998. Trace gas emissions from a north Wales fen-role of
591 hydrochemistry and soil enzyme activity. Water, Air, and Soil Pollution 105, 107-116.
592 Khalil, K., Mary, B., Renault, P., 2004. Nitrous oxide production by nitrification and
593 denitrification in soil aggregates as affected by O2 concentration. Soil Biology and Biochemistry 36, 687-
594 699.
595 Kim, K., Guber, A., Rivers, M., Kravchenko, A., 2020, Contribution of decomposing plant roots
596 to N2O emissions by water absorption, Geoderma 375, 114506.

Kravchenko, A., Toosi, E., Guber, A., Ostrom, N., Yu, J., Azeem, K., Rivers, M., Robertson, G., 2017. Hotspots of soil N 2 O emission enhanced through water absorption by plant residue. Nature Geoscience 10, 496-500.

Kravchenko, A., Fry, J. and Guber, A., 2018. Water absorption capacity of soil-incorporated plant leaves can affect N2O emissions and soil inorganic N concentrations. Soil Biology and Biochemistry. 121, 113-119.

Kuzyakov, Y., Blagodatskaya, E., 2015. Microbial hotspots and hot moments in soil: concept & review. Soil Biology and Biochemistry 83, 184-199.

Li, X., Sørensen, P., Olesen, J.E., Petersen, S.O., 2016. Evidence for denitrification as main source of N2O emission from residue-amended soil. Soil Biology and Biochemistry 92, 153-160.

Liengaard, L., Figueiredo, V., Markfoged, R., Revsbech, N.P., Nielsen, L.P., Prast, A.E., Kühl, M., 2014. Hot moments of N2O transformation and emission in tropical soils from the Pantanal and the Amazon (Brazil). Soil Biology and Biochemistry 75, 26-36.

Loecke, T.D., Robertson, G.P., 2009. Soil resource heterogeneity in terms of litter aggregation promotes nitrous oxide fluxes and slows decomposition. Soil Biology and Biochemistry 41, 228-235.

Markfoged, R., Nielsen, L.P., Nyord, T., Ottosen, L.D.M., Revsbech, N.P., 2011. Transient N2O accumulation and emission caused by O2 depletion in soil after liquid manure injection. European Journal of Soil Science 62, 541-550.

McKenney, D., Drury, C., Wang, S., 2001. Effects of oxygen on denitrification inhibition, repression, and derepression in soil columns. Soil Science Society of America Journal 65, 126-132.

Meyer, R.L., Allen, D.E., Schmidt, S., 2008. Nitrification and denitrification as sources of sediment nitrous oxide production: A microsensor approach. Marine Chemistry 110, 68-76.

Millar, N., Baggs, E., 2004. Chemical composition, or quality, of agroforestry residues influences N2O emissions after their addition to soil. Soil Biology and Biochemistry 36, 935-943.

Milliken, G.A., Johnson, D.E., 2009. Analysis of messy data volume 1: designed experiments. CRC Press.

Morley, N. and Baggs, E., 2010. Carbon and oxygen controls on N2O and N2 production during nitrate reduction. Soil Biology and Biochemistry. 42, 1864-1871.

Myrold, D.D., Tiedje, J.M., 1985. Establishment of denitrification capacity in soil: effects of carbon, nitrate and moisture. Soil Biology and Biochemistry 17, 819-822.

Nagahashi, G., Baker, A.F., 1984. β-Glucosidase activity in corn roots: Problems in subcellular fractionation. Plant physiology 76, 861-864.

Negassa, W.C., Guber, A.K., Kravchenko, A.N., Marsh, T.L., Hildebrandt, B., Rivers, M.L., 2015. Properties of soil pore space regulate pathways of plant residue decomposition and community structure of associated bacteria. PLoS one 10.

Nielsen, L.P., Christensen, P.B., Revsbech, N.P., Sørensen, J., 1990. Denitrification and oxygen respiration in biofilms studied with a microsensor for nitrous oxide and oxygen. Microbial ecology 19, 63-72.

Oates, L.G., Duncan, D.S., Gelfand, I., Millar, N., Robertson, G.P., Jackson, R.D., 2016. Nitrous oxide emissions during establishment of eight alternative cellulosic bioenergy cropping systems in the North Central United States. Gcb Bioenergy 8, 539-549.

Parkin, T.B., 1987. Soil microsites as a source of denitrification variability 1. Soil Science Society of America Journal 51, 1194-1199.

Parkin, T.B., 1987. Soil microsites as a source of denitrification variability 1. Soil Science Society of America Journal 51, 1194-1199.

Parsons, L.L., Smith, M.S., Murray, R.E., 1991. Soil denitrification dynamics: spatial and temporal variations of enzyme activity, populations, and nitrogen gas loss. Soil Science Society of America Journal 55, 90-95.

Partey, S., Preziosi, R., Robson, G., 2014. Improving maize residue use in soil fertility restoration by mixing with residues of low C-to-N ratio: effects on C and N mineralization and soil microbial biomass. Journal of soil science and plant nutrition 14, 518-531.

Razavi, B.S., Zarebanadkouki, M., Blagodatskaya, E., Kuzyakov, Y., 2016. Rhizosphere shape of lentil and maize: spatial distribution of enzyme activities. Soil Biology and Biochemistry 96, 229-237.

Revsbech, N., Pedersen, O., Reichardt, W., Briones, A., 1999. Microsensor analysis of oxygen and pH in the rice rhizosphere under field and laboratory conditions. Biology and fertility of soils 29, 379-385.

Revsbech, N.P., Nielsen, L.P., Christensen, P.B., Sørensen, J., 1988. Combined oxygen and nitrous oxide microsensor for denitrification studies. Applied and environmental microbiology 54, 2245-2249.

Riederer, M. and Schreiber, L., 2001. Protecting against water loss: analysis of the barrier properties of plant cuticles. Journal of experimental botany. 52, 2023-2032.

Rohe, L., Apelt, B., Vogel, H.-J., Well, R., Wu, G.-M., Schlüter, S., 2020. Denitrification in soil as a function of oxygen supply and demand at the microscale. Biogeosciences Discussions, 1-32.

Schimel, J., Becerra, C.A., Blankinship, J., 2017. Estimating decay dynamics for enzyme activities in soils from different ecosystems. Soil Biology and Biochemistry 114, 5-11.

Senbayram, M., Chen, R., Budai, A., Bakken, L., Dittert, K., 2012. N2O emission and the N2O/(N2O+ N2) product ratio of denitrification as controlled by available carbon substrates and nitrate concentrations. Agriculture, Ecosystems & Environment 147, 4-12.

Sinsabaugh, R.L., Lauber, C.L., Weintraub, M.N., Ahmed, B., Allison, S.D., Crenshaw, C., Contosta, A.R., Cusack, D., Frey, S., Gallo, M.E., 2008. Stoichiometry of soil enzyme activity at global scale. Ecology letters 11, 1252-1264.

Smith, M.S., Tiedje, J.M., 1979. Phases of denitrification following oxygen depletion in soil. Soil Biology and Biochemistry 11, 261-267.

Spohn, M., Carminati, A., Kuzyakov, Y., 2013. Soil zymography–a novel in situ method for mapping distribution of enzyme activity in soil. Soil Biology and Biochemistry 58, 275-280.

Steffens, C., Helfrich, M., Joergensen, R.G., Eissfeller, V., Flessa, H., 2015. Translocation of 13C-labeled leaf or root litter carbon of beech (Fagus sylvatica L.) and ash (Fraxinus excelsior L.) during decomposition–A laboratory incubation experiment. Soil Biology and Biochemistry 83, 125-137.

Toosi, E., Kravchenko, A., Guber, A., Rivers, M., 2017. Pore characteristics regulate priming and fate of carbon from plant residue. Soil Biology and Biochemistry 113, 219-230.

Uselman, S.M., Qualls, R.G. and Lilienfein, J., 2012. Quality of soluble organic C, N, and P produced by different types and species of litter: Root litter versus leaf litter. Soil Biology and Biochemistry. 54, 57-67.

Wallenstein, M.D. and Weintraub, M.N., 2008. Emerging tools for measuring and modeling the in situ activity of soil extracellular enzymes. Soil Biology and Biochemistry. 40, 2098-2106.

682 Wang, J.J., Tharayil, N., Chow, A.T., Suseela, V. and Zeng, H., 2015. Phenolic profile within the
683 fine- root branching orders of an evergreen species highlights a disconnect in root tissue quality predicted
684 by elemental- and molecular- level carbon composition. New Phytologist. 206, 1261-1273.
685 Wu, D., Wei, Z., Well, R., Shan, J., Yan, X., Bol, R. and Senbayram, M., 2018. Straw amendment
686 with nitrate-N decreased N2O/(N2O+ N2) ratio but increased soil N2O emission: A case study of direct
687 soil-born N2 measurements. Soil Biology and Biochemistry. 127, 301-304.

688 Yeats, T.H. and Rose, J.K., 2013. The formation and function of plant cuticles. Plant physiology.
689 163, 5-20.

690 Zhang, D., Hui, D., Luo, Y., Zhou, G., 2008. Rates of litter decomposition in terrestrial
691 ecosystems: global patterns and controlling factors. Journal of Plant Ecology 1, 85-93.

Table 1. Total carbon and nitrogen contents in the plant residues.

Plant type	Carbon (w %)***	Nitrogen (w %)***	C:N ratio***
Leaf	44.2 (0.54)	1.90 (0.17)	24.0 (2.5)
Root	47.4 (0.40)	0.58 (0.08)	82.7 (12.1)

*** indicates significant differences between leaf and roots ($p < 0.01$).

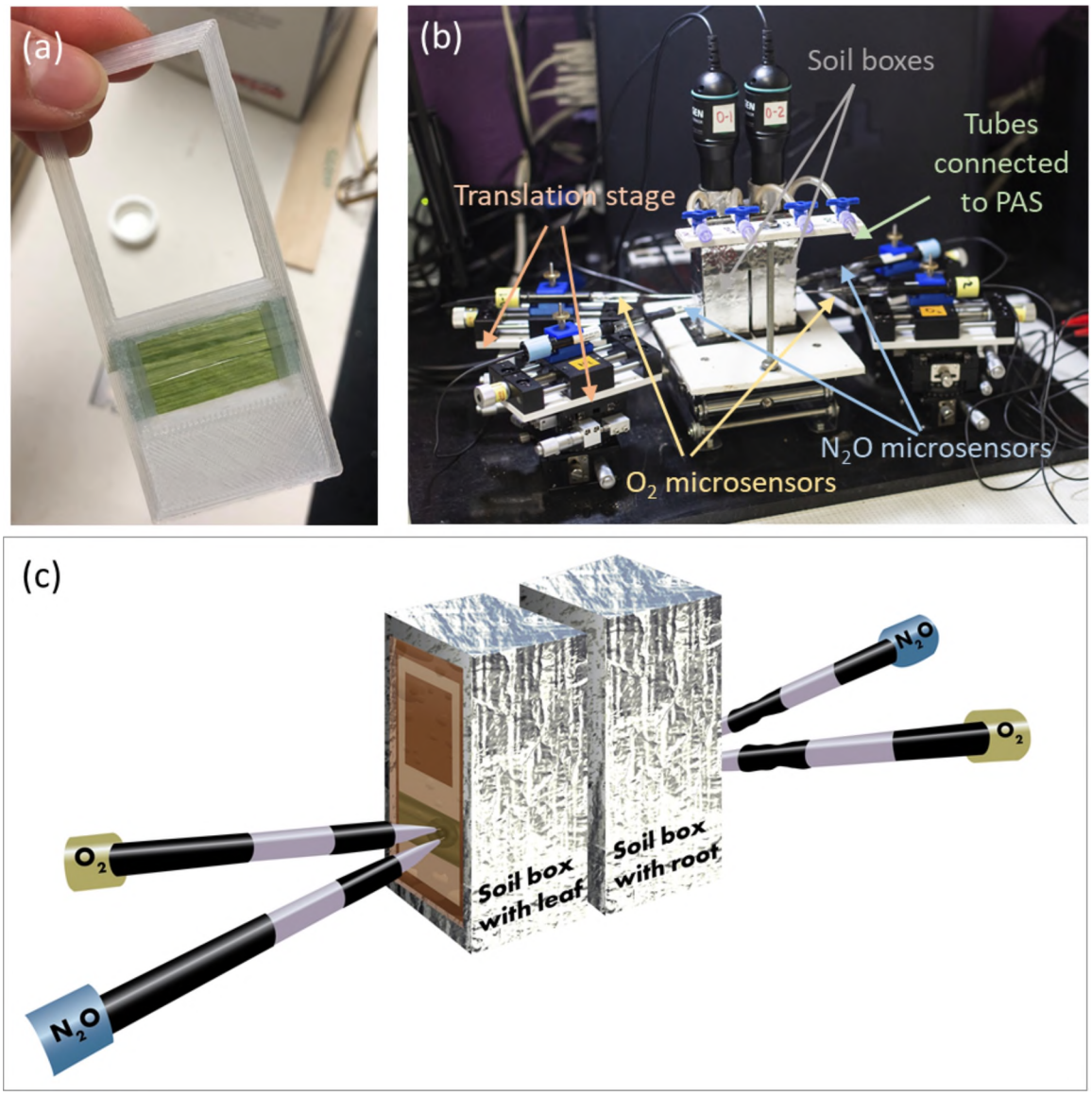

Figure 1. Experimental setup for microsensor measurements. (a) Flattened residue fragments in the holder. Holder was used to fix the location of residue fragments in the soil box. (b) The experimental setup. It shows boxes containing soil with incorporated residues, microsensors inserted into the boxes, and tubing connecting the air chambers above the soil boxes with the PAS device for measuring air concentrations of N_2O and CO_2. (c) Schemetic representation of the microsensor locations in vicinity to the residue within the soil box.

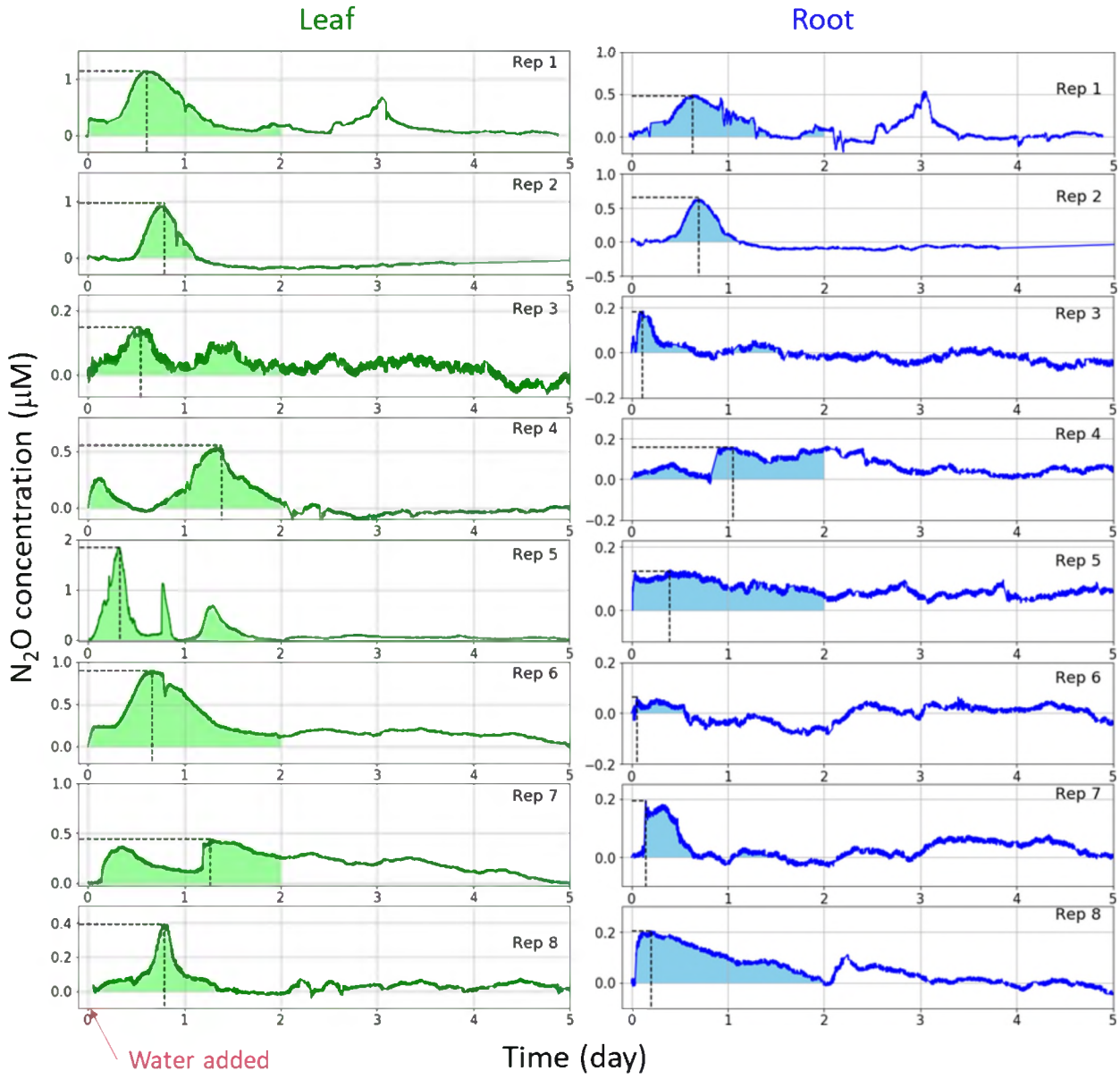

Figure 2. Dynamics of N_2O concentrations in the soil microcosms with (a) leaf and (b) root residues. Black dotted lines indicate the timepoint at which the lag time and the peak (maximum) concentration were determined. Colored area under each curve presents cumulative N_2O production for 2 days. Red circles mark an example of artificial fluctuations in one of the experimental runs.

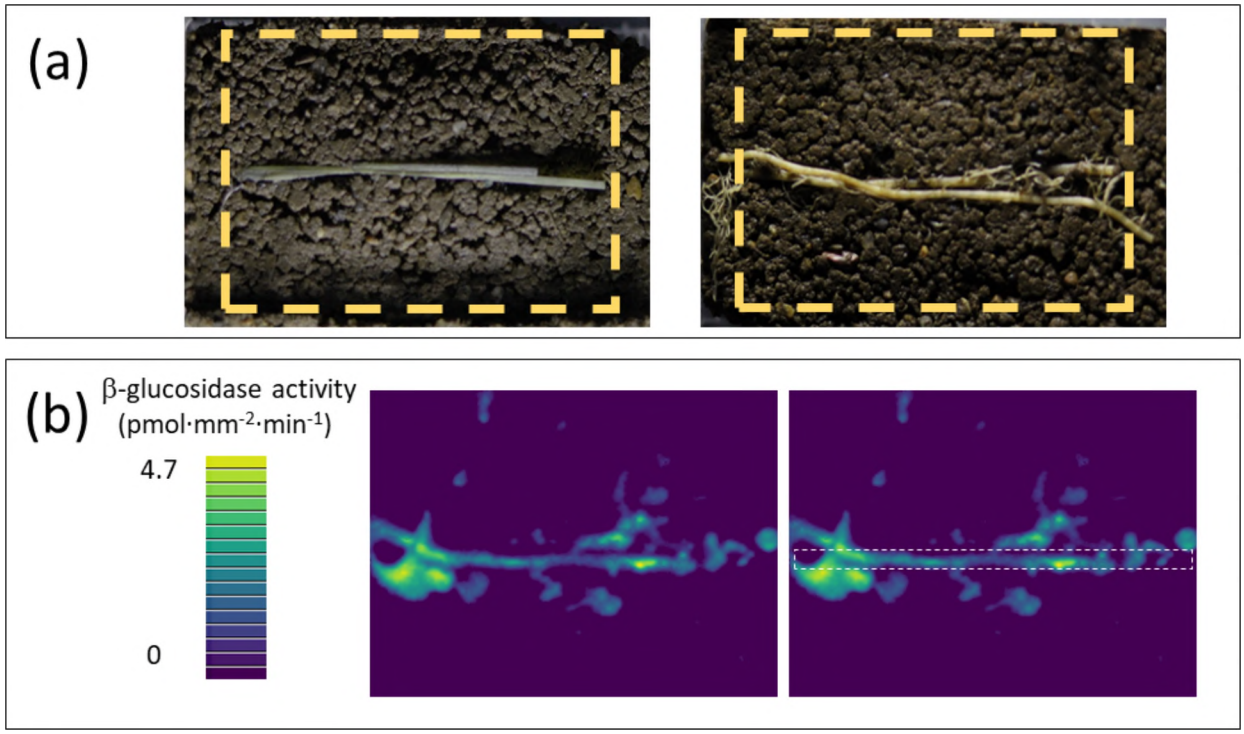

Figure 3. Examples of (a) boxes with soil and plant residues used for soil zymography and (b) resultant zymography images. Yellow dotted rectangles on (a) mark the areas that were subjected to zymography, i.e., membrane placement. The white dotted rectangle on (b) encompasses the area used to calculate the enzyme activity for the incubated plant residue.

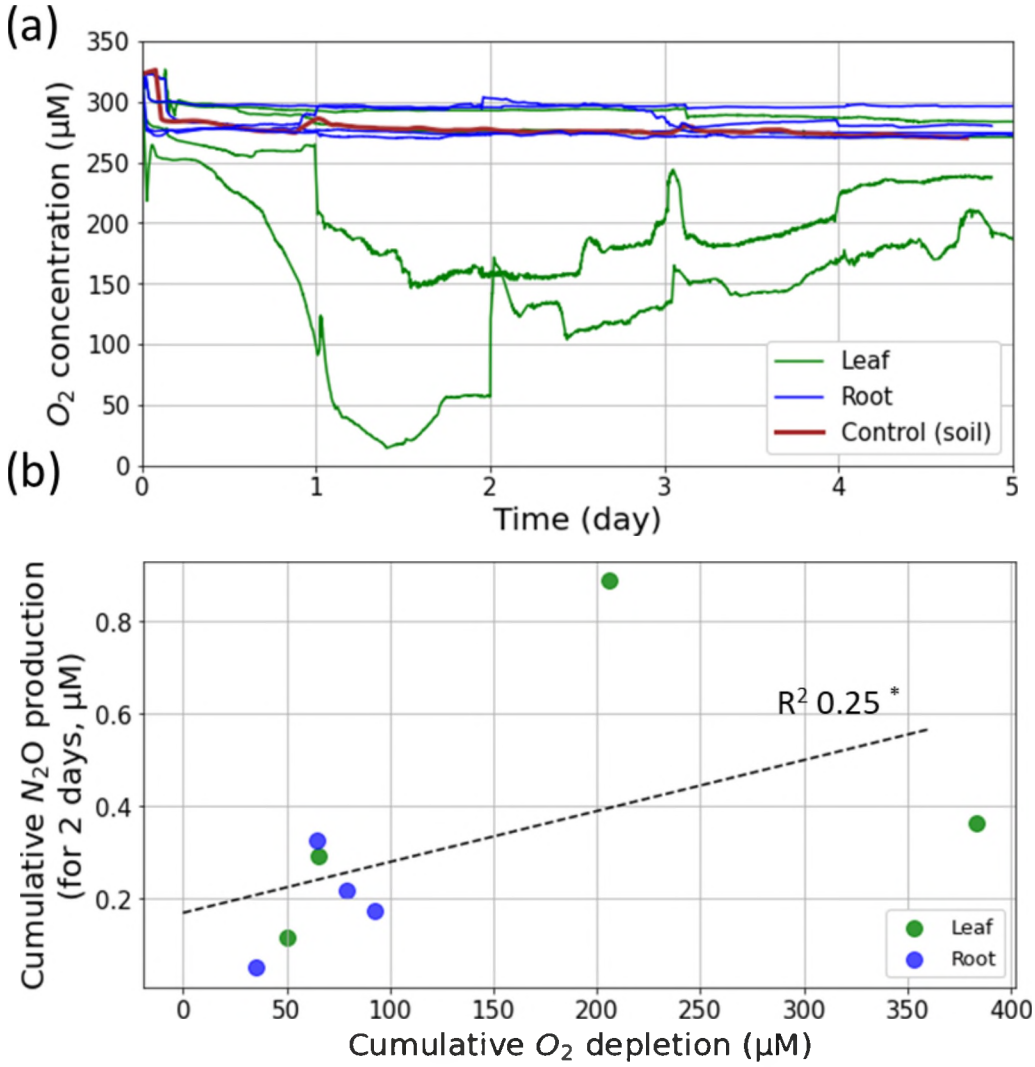

Figure 4. (a) Microsensor recorded O_2 concentrations near switchgrass residues and control soil during the experiment. Water addition started at time 0. (b) Cumulative O_2 depletion plotted vs. cumulative N_2O production during the first 2 days of the experiment. Dotted line is the linear regression model fitted to the data ($p < 0.10$, one-tailed test).

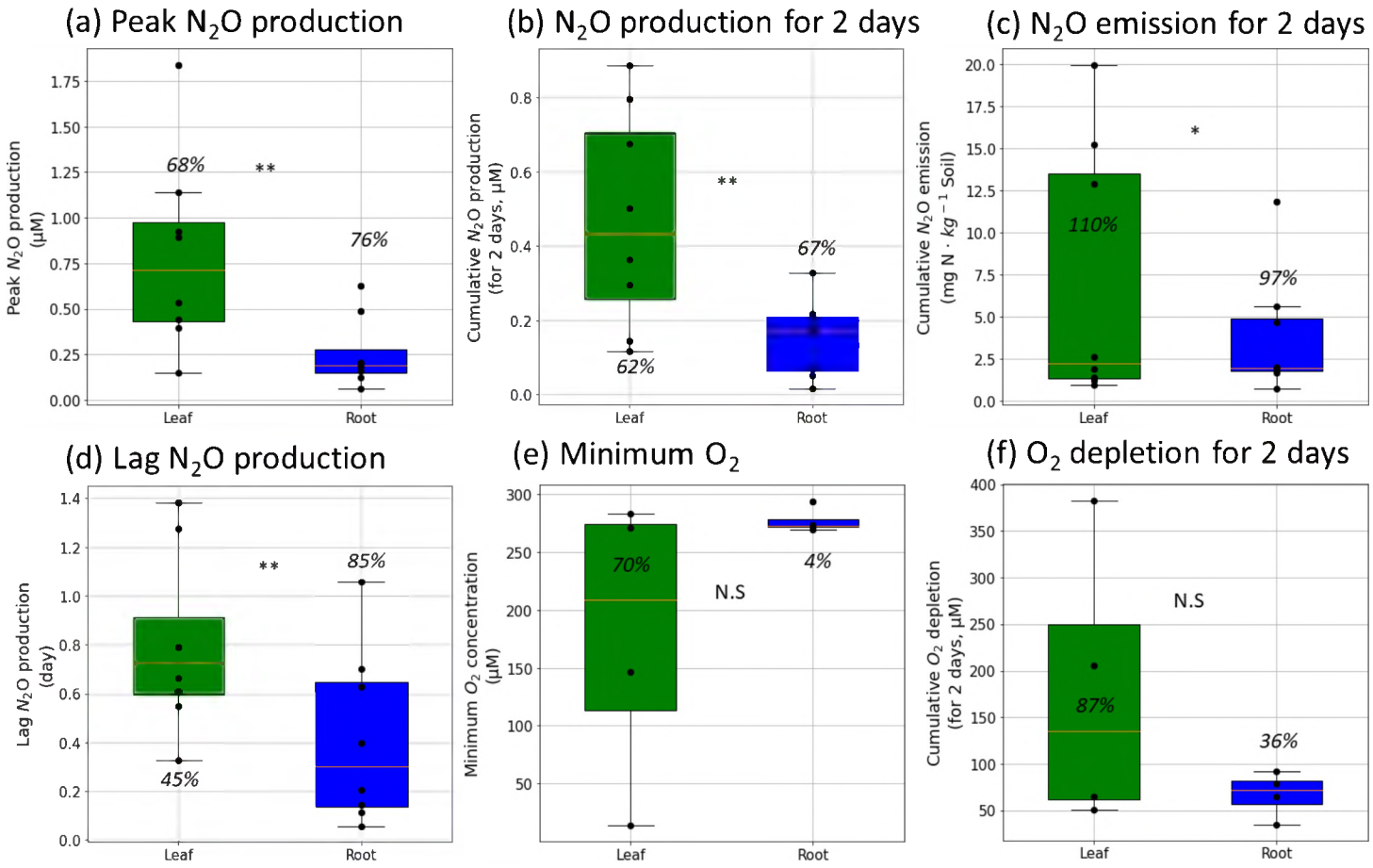

Figure 5. Boxplot of quantitative measurements from microsensor and Photoacoustic Spectroscopy. (a) Peak N_2O production - the maximum N_2O concentration observed from 5 days of microcensor recordings, (b) Cumulative N_2O production - the area under the microsensor curves and above zero for 2 days, (c) N_2O emission –N_2O from the surface of the soil measured from headspace, (d) lag N_2O production – the time elaped from the start of the soil wetting until the peak production, (e) minumum O_2 concentration - the lowest O_2 concentration observed from 5 days of microcensor recordings, and (f) O_2 depletion for 2 days - the area under the base O_2 concentration. ** and * indicate significant differences between leaves and roots ($p < 0.05$ and 0.10). Black dots are individual observations from each run. The coefficients of variavtion were presented as percentage.

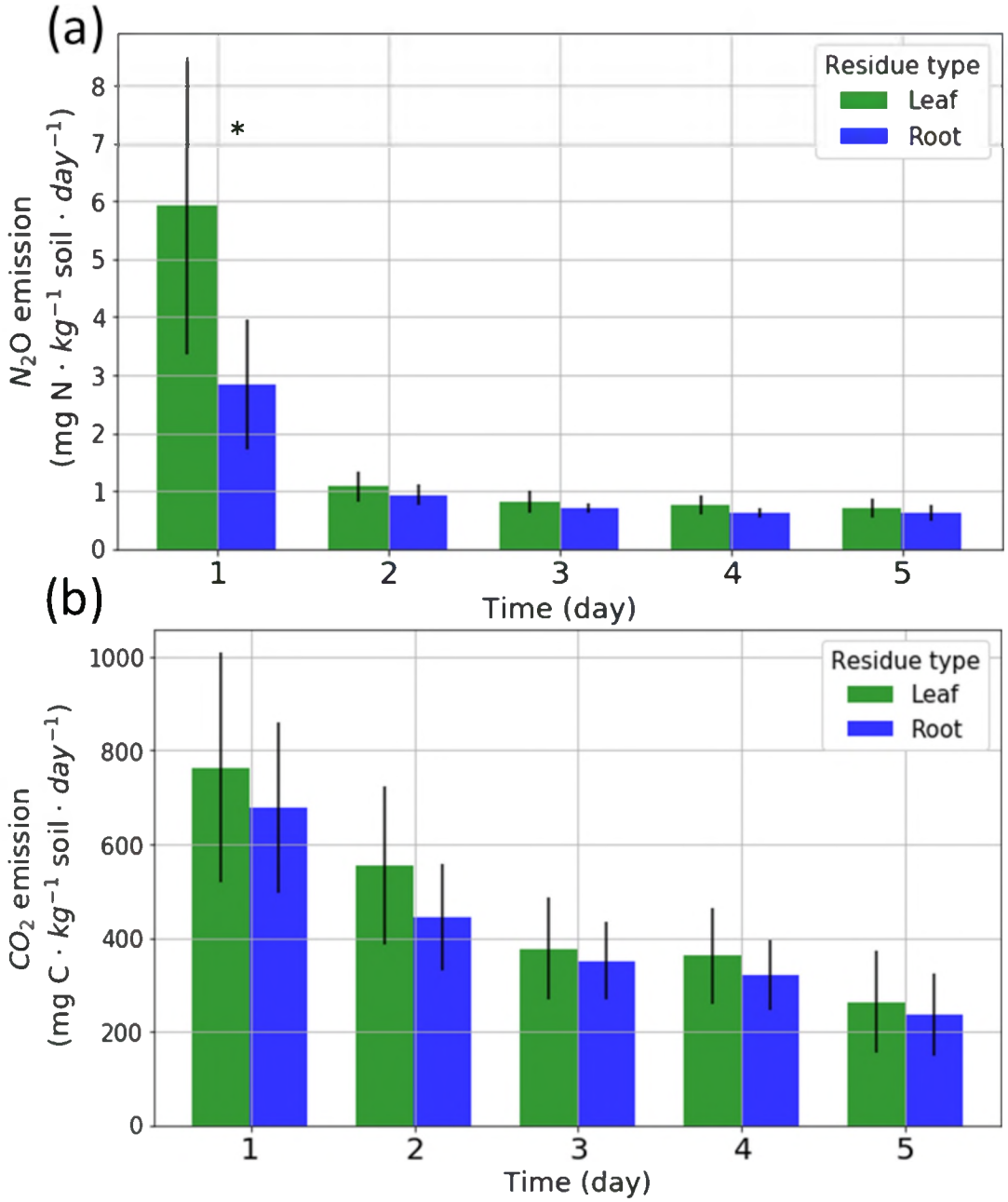

Figure 6. (a) N_2O and (b) CO_2 emission rates from the soil boxes with incorporated leaf and root residues, measured using Photoacoustic Spectroscopy. Vertical lines represent standard errors. * indicates significant differences between leaves and roots ($p < 0.10$).

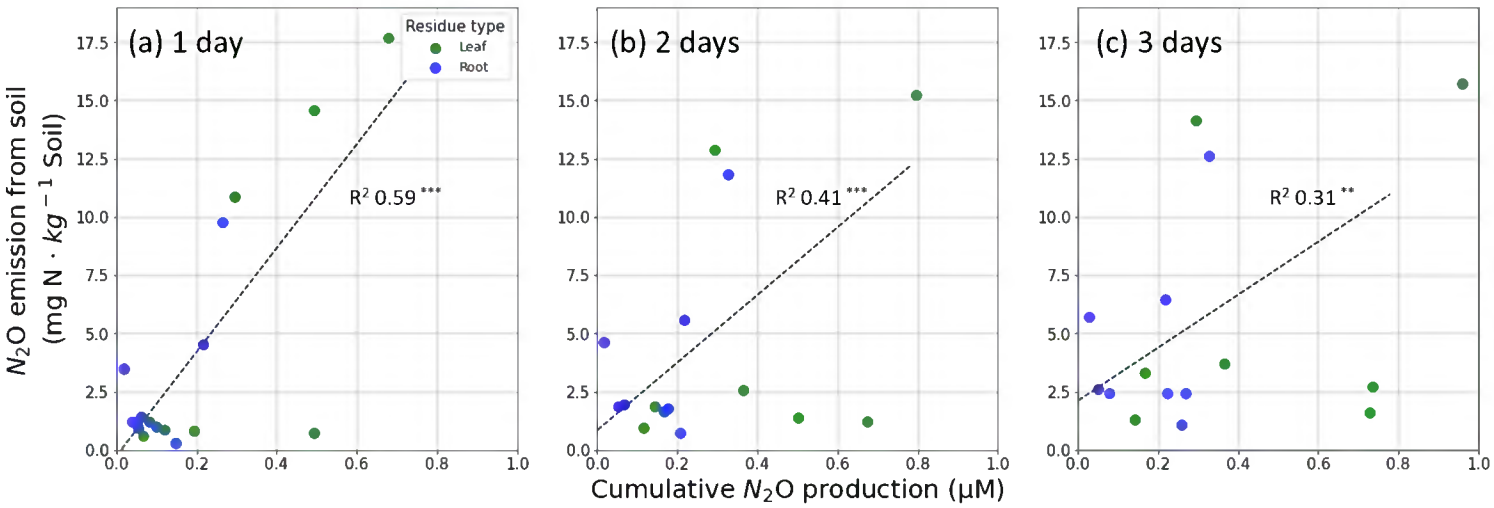

Figure 7. Relationship between cumulative N_2O productions (measured from soil pore using microsensor) in and emissions (measured from headspace using photoacoustic spectroscopy) from the microcosms (a) for 1 day, (b) 2 days, and (c) 3 days of the experiment. Dotted lines represent linear regression models. All regressions were statistically significant at $p < 0.01$ and $p < 0.05$ (marked with *** and **). There were no significant differences between regression slopes of leaves and roots.

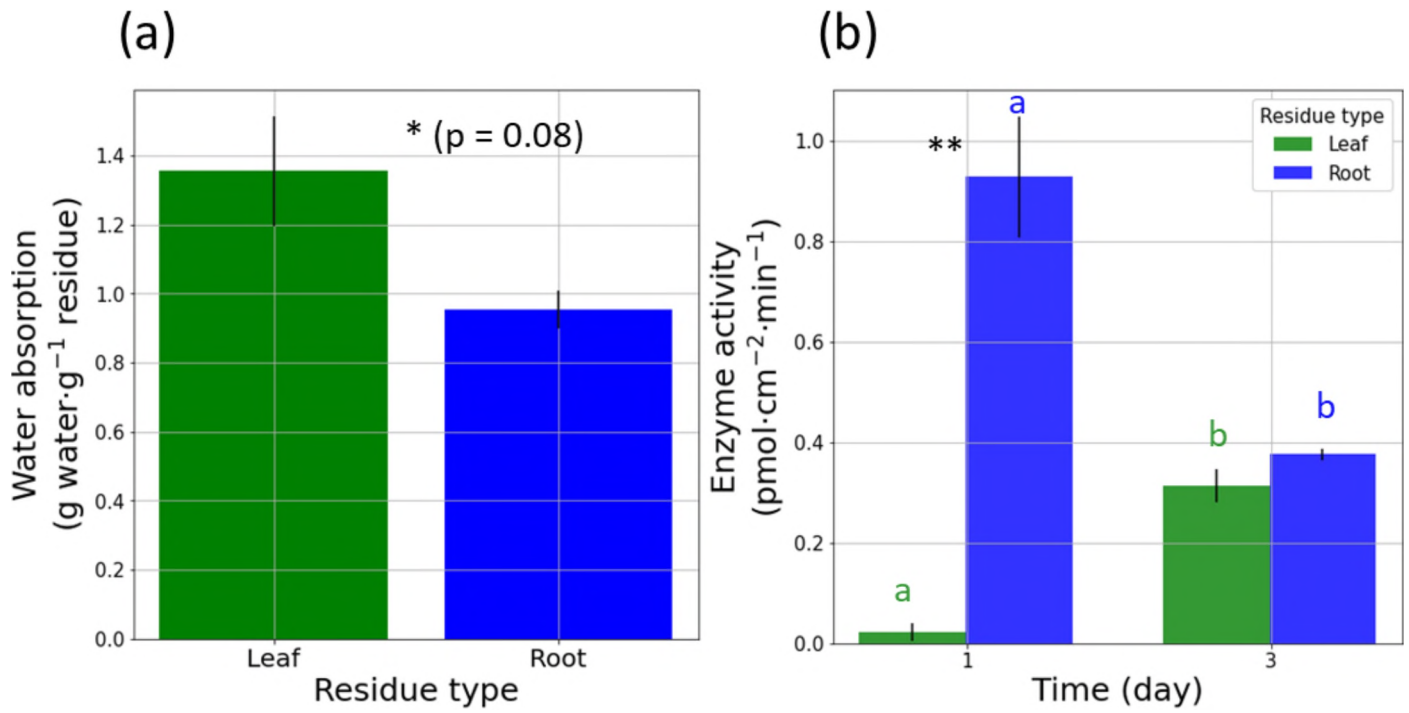

Figure 8. (a) Average water absorption levels by leaf and root residues. The difference between leaves and roots is significant at $p < 0.10$. (b) Average enzyme (β-glucosidase) activity at the surface of the plant residues at day 1 and 3 of the experiment. Different letters mark significant differences between the days within each residue type ($p < 0.10$). Symbol ** indicates the significant differences between residue types at a given day ($p < 0.05$). Vertical lines represent standard errors.